# Synthesis of a Tetracorannulene-Perylenediimide that Acts as a Selective Receptor for $C_{60}$ over $C_{70}$

Víctor García-Calvo,[†] José V. Cuevas,[†] Héctor Barbero,[‡] Sergio Ferrero,[‡] Celedonio M. Álvarez,[‡] Jesús A. González,[§] Borja Díaz de Greñu,[†] José García-Calvo,[†] and Tomás Torroba*[,†].

[†] Departamento de Química, Facultad de Ciencias, Universidad de Burgos, 09001 Burgos, Spain

[‡] MIOMeT, CINQUIMA/Química Inorgánica, Facultad de Ciencias, Universidad de Valladolid, E-47011, Valladolid, Spain.

[§] Departamento CITIMAC, Universidad de Cantabria, 39005 Santander, Spain.

*Supporting Information*

**ABSTRACT:** We report the use of a tetraborylated perylenediimide as starting material for the preparation of a tetracorannulene-perylenediimide that is able to bind up to two fullerene-$C_{60}$ molecules by host-guest molecular recognition with preference over $C_{70}$. Titration with fullerene-$C_{60}$ is followed by a dramatic shift of the aromatic signals in $^1$H NMR and an initial increase in the fluorescence of the system. By this simple mechanism, fluorogenic sensing of fullerene-$C_{60}$ is easily accomplished by an unprecedented fluorescent turn-on mechanism.

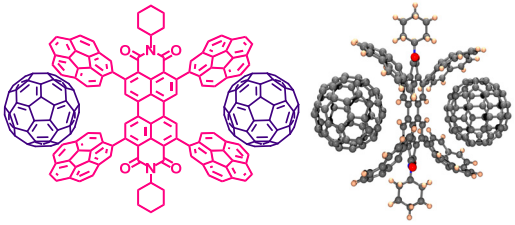

The host-guest molecular recognition of corannulene[1] and fullerenes of diverse size and shape is one of the landmarks of the supramolecular chemistry of curved hydrocarbons.[2] The bowl-shaped concave corannulene complexes the balloon shape fullerenes by π-π stacking and this interaction was used for effective cocrystalization,[3] and characterization;[4] it was frequently used for the construction of molecular devices[5] such as either flexible or rigid molecular tweezers bearing two corannulene subunits.[6] They compete in affectivity with a large variety of heterogeneous molecular tweezers and curved traps of fullerene derivatives.[7] On the other hand, perylenediimides are strongly fluorescent compounds,[8] stable under light and air, so they are good candidates for the search of new fluorogenic reporters of important analytes when bonded to polymeric materials,[9] silica nanoparticles,[10] or magnetic beads.[11] Remarkable corannulene-perylenediimide derivatives have been described, bearing up to five perylenediimide units per corannulene,[12] or two corannulene units in a perylenediimide scaffold.[13] We have described flexible tetraarylporphyrins containing four corannulene units,[14] now we have focused into the use of a perylenediimide as starting material for the preparation of an unprecedented rigid tetracorannulene-perylenediimide derivative with cavities designed to be able to bind up to two fullerene-$C_{60}$ molecules by host-guest molecular recognition. The synthesis was straightforward by the palladium(0)-catalyzed Suzuki reaction of bromocorannulene[15] and a tetraborylated perylenediimide PDI(BPin)$_4$, in turn prepared by the iridium-catalyzed direct tetraborylation[16] of the *N,N'*-dicyclohexylperylenediimide[10] (Scheme 1). Work-up and column chromatography gave the dark red fluorescent compound PDI(Cor)$_4$ in 74% yield ($\lambda_{max.}$= 460, 491, 528, $\varepsilon_{528}$ = 15269 $M^{-1}cm^{-1}$, $\lambda_{em.}$= 522, 562, 613, φ = 0.55, τ = 4.71 ns, toluene). $^1$H NMR titration of PDI(Cor)$_4$ 10 μM in toluene-D8 with $C_{60}$ showed a dramatic shift of some aromatic signals (Figure 1), the most pronounced shift for the 7.74 ppm signal.

Scheme 1

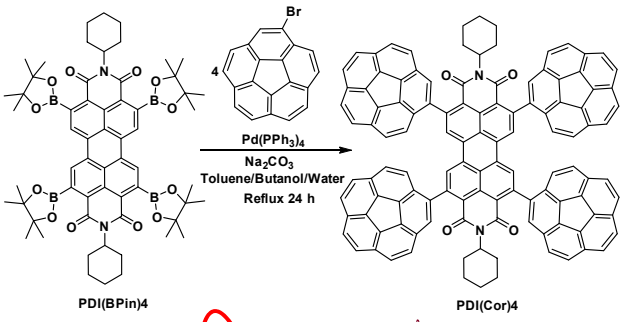


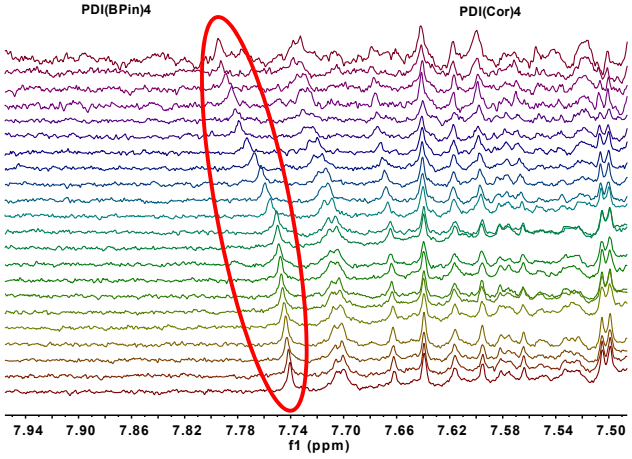


**Figure 1** $^1$H NMR titration of PDI(Cor)$_4$ and $C_{60}$ in toluene-D8.

A similar titration experiment with $C_{70}$ afforded a less pronounced signal shift (Figure 2), therefore showing a marked preference for complexation of $C_{60}$.

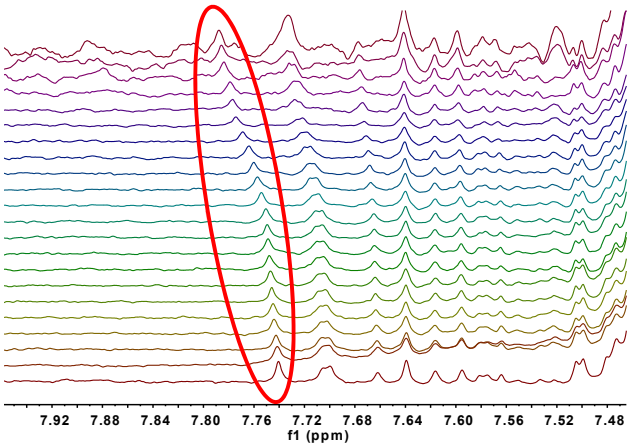


**Figure 2** $^1$H NMR titration of PDI(Cor)$_4$ and $C_{70}$ in toluene-D8.

Plotting the experimental displacements and fitting the points to appropriate models gave a good estimation from a 1:2 additive model,[17] affording complexation constants: $K_1$ = 4700 (±200) and $K_2$ = 2800 (±400) for PDI(Cor)$_4$ and $C_{60}$ and $K_1$ = 1590 (±50) and $K_2$ = 220 (±190) for PDI(Cor)$_4$ and $C_{70}$, thus confirming the selectivity and much higher affinity for complexation of PDI(Cor)$_4$ and $C_{60}$ over $C_{70}$ (Figure 3).

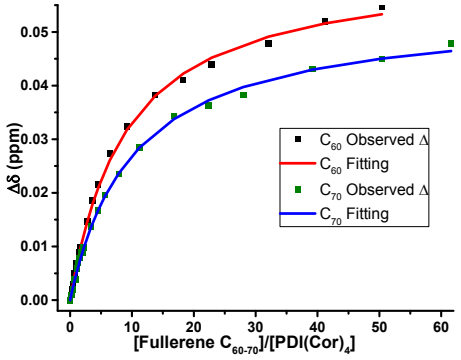


**Figure 3** $^1$H NMR titration plots and curve fittings of PDI(Cor)$_4$ and $C_{60}$ (red) or $C_{70}$ (blue) in toluene-D8, 7.73→7.78 ppm signal.

The extreme complexity of the NMR spectra (see the Supporting information) precluded a simple explanation for the interaction between PDI(Cor)$_4$ and $C_{60}$ by NMR spectroscopy. To shed light on this interaction we performed DFT calculations of structures involved in the interaction. Quantum chemical calculations were performed using the DFT functional M06-2X developed by Zhao and Trular because this functional accounts for the noncovalent interactions.[18] The basis set used in the definition of the atoms were the Pople bases 6-31G*. The calculations were performed using the Gaussian 09 package software.[19] Minimization of PDI(Cor)$_4$ gave seven minimum point structures with related energies (energy differences up to 3 Kcal/mol) coming from atropisomers of the four corannulene units. The most suitable structure to receive the fullerenes was then subjected to DFT modelization as complexes with one and two fullerene-$C_{60}$ units, the results are shown in Figure 4. Albeit the 1:1 complex gave a single minimized structure, the addition of a new $C_{60}$ unit gave two independent diastereoisomers, the "cis" and "trans" isomers shown in Figure 4, being the cis isomer more stable than the trans isomer by about 4 Kcal/mol.

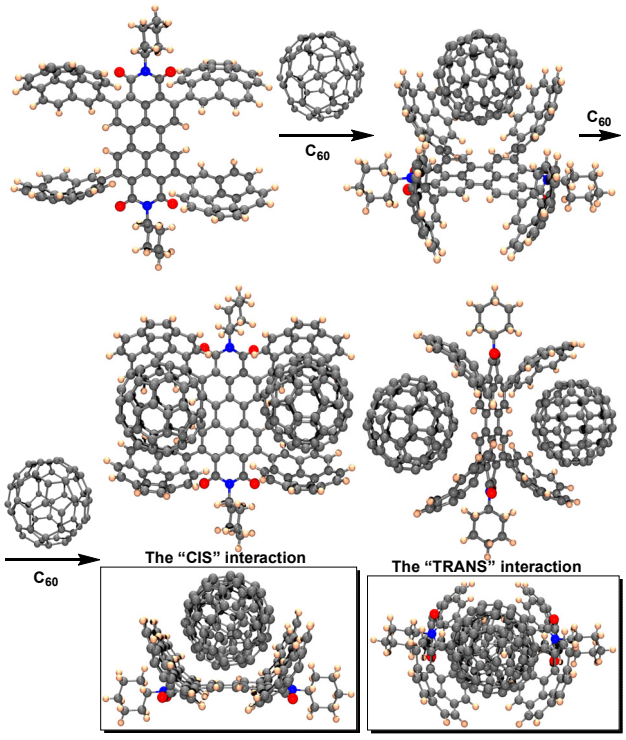


**Figure 4** DFT calculated structures of complexes PDI(Cor)$_4$[$C_{60}$]$_{1\text{-}2}$. In boxes, different orientations of the cis and trans diastereoisomers.

Being fluorescent in solution, PDI(Cor)$_4$ permitted titrations with $C_{60}$ by fluorescence spectroscopy (Figures 5-6).

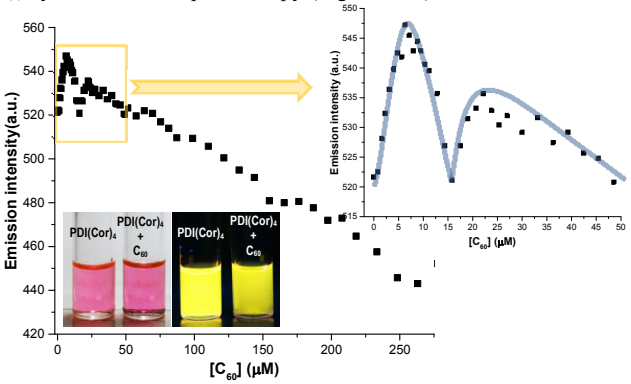


**Figure 5** Fluorescence titration plot of PDI(Cor)$_4$ and $C_{60}$ in $CHCl_3$ and images of solutions of PDI(Cor)$_4$ in $CHCl_3$ and PDI(Cor)$_4$ with excess $C_{60}$ in $CHCl_3$ under white light and 366 nm light. Inset: amplification of the titration plot and tendency line.

Thus, fluorescent titration of PDI(Cor)$_4$, 10 μM in chloroform solution, with successive additions of $C_{60}$, $\lambda_{exc}$ = 485 nm, $\lambda_{em}$ = 540 nm, and plotting of the maximum peak evolution, gave a titration plot (Figure 5) in which the initial points of the titration plot gave an unexpected pattern of initial increase of fluorescence until 0.5 equivalents of $C_{60}$ are added, then a decrease of fluorescence until 1.5 equivalents of $C_{60}$ are added, then a new increase of fluorescence until 2-2.5 equiv $C_{60}$ are added (Figure 5 inset) and then a continuous decrease of fluorescence along the rest of the titration by the quenching effect of $C_{60}$. The observed behavior is repeatable and did not depend on time, solvent or concentration. For instance, the fluorescent titration plot of PDI(Cor)$_4$, 5 μM in toluene solution by successive additions of $C_{60}$, $\lambda_{exc}$ = 490 nm, $\lambda_{em}$

= 525 nm, from 0 to 30 μM $C_{60}$, afforded a similar behavior, the initial points of the titration plot gave an initial increase of fluorescence, reaching a maximum when 0.5 equivalents of $C_{60}$ were added, then the fluorescence decreased to the initial value when 1.5 equivalents of $C_{60}$ were added, after that a new increase of fluorescence with successive additions of $C_{60}$ was recorded, reaching the previous maximum when 2.5-3 equivalents of $C_{60}$ were added, then a continuous decrease of fluorescence along the rest of titration was recorded (Figure 6).

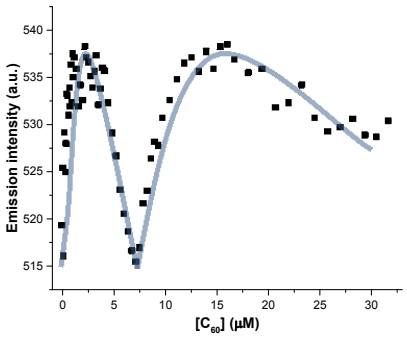


**Figure 6** Fluorescence titration plot of $PDI(Cor)_4$ and $C_{60}$ in toluene. In grey color, the tendency line of the plot.

The unusual behavior showed by the titration plots can be interpreted in terms of two competing mechanisms, complexation and quenching, occurring simultaneously (Scheme 2).

Scheme 2

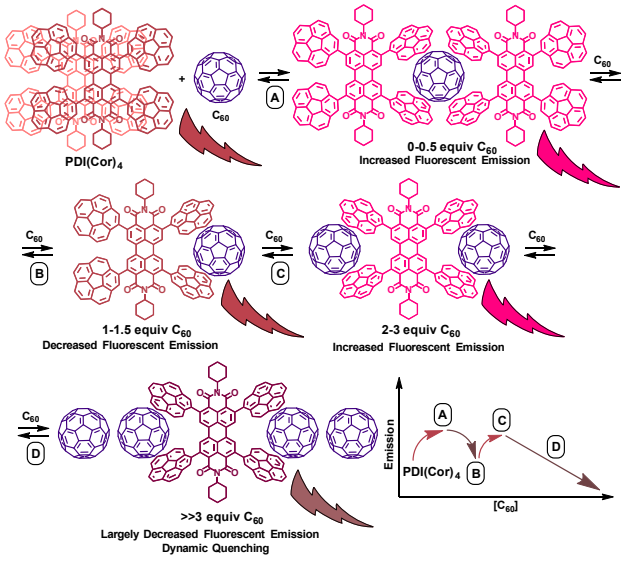


Successive addition of $C_{60}$ probably starts some disaggregation of $PDI(Cor)_4$ as $C_{60}$ complexation occurs, with increased fluorescent emission, until the 1:1 complex is formed that triggers a decreased fluorescent emission to the initial state. Then, the formation of the 1:2 complex gives rise to an increase in the fluorescence of the system and further addition of $C_{60}$ gives rise to decreased fluorescent emission by dynamic quenching (Scheme 2). By this simple mechanism, fluorogenic sensing of fullerene-$C_{60}$ was easily accomplished by an unprecedented fluorescent turn-on mechanism. Further confirmation of the molecular interaction between $PDI(Cor)_4$ and $C_{60}$ was studied by high pressure Raman spectroscopy. Unpolarized Raman-scattering measurements were performed in a membrane diamond-anvil cell where the pressure can be varied by pneumatic bellows. Liquid chloroform was used as pressure transmitting media. The pressure was calibrated to within 0.1 GPa by using the power five ruby luminescence scale with the pressure in GPa related to the wavelength λ, by $P = 380.8\{[\lambda/\lambda_0]^{5}-1\}$.[20] The ruby samples were ~4000 ppm $Cr^{3+}$ doped and 5-15 μm in average dimensions. It must be noted, however, that according to the ruby line broadening, non-hydrostatic effects were insignificant in the explored range. The Raman spectra were taken by using the 514.5-nm line of an $Ar^+$-$Kr^+$ laser and nitrogen-cooled CCD with a confocal microscope for detection, in the backscattering geometry. The laser spot was 20 μm in diameter. In the cell a power of 5 mW incident on the diamonds proved to be low enough not to cause any heating of the sample in the pressurizing medium. The resolution was better than 1 $cm^{-1}$. The Raman dependence with pressure of a sample of $PDI(Cor)_4$ and $C_{60}$ in chloroform is shown in Figure 7.

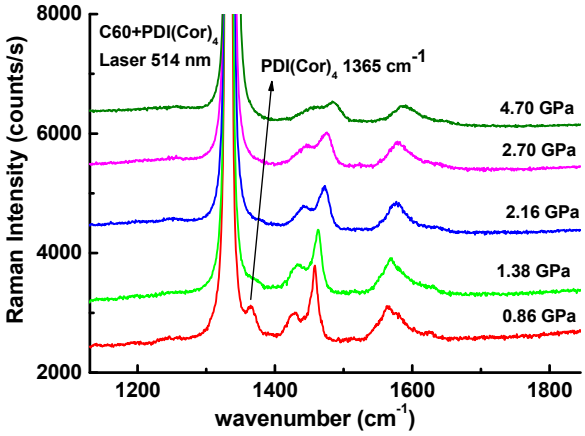


**Figure 7** Raman dependence with pressure of a sample of $PDI(Cor)_4$ and $C_{60}$ in chloroform.

A characteristic signal of the $PDI(Cor)_4$, the vibration mode of 1365 $cm^{-1}$, is observed in the sample $PDI(Cor)_4$ + $C_{60}$ at low pressures but it is clearly observed how this frequency disappears between 2.16 and 2.70 GPa. The vibration mode at 1365 $cm^{-1}$ does not disappear with the pressure in the $PDI(Cor)_4$ sample alone. The dependence with pressure of the individual sample of $PDI(Cor)_4$ and the one of $C_{60}$[21] is shown in the supporting information. The theoretical analysis of the calculated vibrational frequencies of the most stable atropisomer of $PDI(Cor)_4$ shows how at about 1385–1392 $cm^{-1}$ some vibrational signals appear that belong to in-plane bending vibrations of the C-H bonds of the bay position of the perylene fragment, as well as similar vibrations of C-H bonds of corannulene moieties. These vibrations seem to be very sensitive to the interaction with $C_{60}$ molecules because of the close proximity of bay and corannulene protons to $C_{60}$ in the complex. Therefore the interaction of $PDI(Cor)_4$ and $C_{60}$ is confirmed by the high pressure Raman measurements of mixtures of $PDI(Cor)_4$ and $C_{60}$ by the disappearance of the 1365 $cm^{-1}$ signal, as well as their broadening and displacement, as the interaction is increased under high pressure (Figure 8).

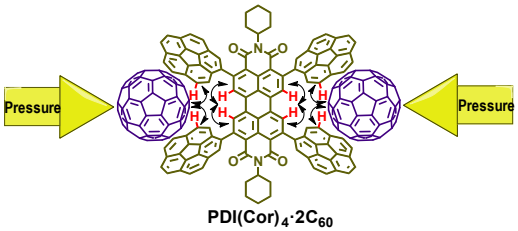


**Figure 8** A cartoon of the hindering of Raman signals with pressure of a sample of $PDI(Cor)_4$ and $C_{60}$ in chloroform.

In conclusion, we have synthesized for the first time a tetracorannulene-perylenediimide that is able to bind up to two fullerene-$C_{60}$ molecules by host-guest molecular recognition. Thus, complexation with fullerene-$C_{60}$ is followed by a dramatic shift of the aromatic signals in $^1$H NMR and an initial increase in the fluorescence of the system. By this simple mechanism, fluorogenic sensing of fullerene-$C_{60}$ is easily accomplished by an unprecedented fluorescent turn-on mechanism. In addition, Raman dependence with pressure of a sample of PDI(Cor)$_4$ and $C_{60}$ in chloroform confirmed the calculated structure of the complex by the disappearance of a characteristic Raman signal, as well as their broadening and displacement, as the interaction between PDI(Cor)$_4$ and $C_{60}$ is increased under high pressure.

## ASSOCIATED CONTENT

### Supporting Information

The Supporting Information is available free of charge on the ACS Publications website.

Synthetic procedures, NMR, HRMS, UV−vis absorption and fluorescence spectra, titration studies, DFT calculations of conformers and inclusion complexes, and Raman dependence with pressure studies (PDF).

## AUTHOR INFORMATION

### Corresponding Author

* E-mail: ttorroba@ubu.es.

### Notes

The authors declare no competing financial interest.

## ACKNOWLEDGMENT

We gratefully acknowledge financial support from the Ministerio de Economía y Competitividad, Spain (Project CTQ2015-71353-R) and Junta de Castilla y León, Consejería de Educación y Cultura y Fondo Social Europeo (Project BU263P18).

## REFERENCES

(1) Reviews: (a) Haupt, A.; Lentz, D. *Chem. Eur. J.* **2019**, *25*, 3440–3454. (b) Li, X.; Kang, F.; Inagaki, M. *Small* **2016**, *12*, 3206–3223. Recent examples: (c) Tian, X.; Roch, L. M.; Vanthuyne, N.; Xu, J.; Baldridge, K. K.; Siegel, J. S. *Org. Lett.* **2019**, DOI: 10.1021/acs.orglett.9b00718. (d) Gallego, M.; Calbo, J.; Calderon, R. M. K.; Pla, P.; Hsieh, Y.-C.; Perez, E. M.; Wu, Y.-T.; Orti, E.; Guldi, D. M.; Martin, N. *Chem. Eur. J.* **2017**, *23*, 3666–3673. (e) Fujikawa, T.; Preda, D. V.; Segawa, Y.; Itami, K.; Scott, L. T. *Org. Lett.* **2016**, *18*, 3992−3995.

(2) Selmani, S.; Schipper, D. J. *Chem. Eur. J.* **2019**, *25*, 6673–6692. (b) Saito, M.; Shinokubo, H.; Sakurai, H. *Mater. Chem. Front.* **2018**, *2*, 635−661. (c) Stępień, M.; Gońka, E.; Żyła, M.; Sprutta, N. *Chem. Rev.* **2017**, *117*, 3479−3716.

(3) (a) Lampart, S.; Roch, L. M.; Dutta, A. K.; Wang, Y.; Warshamanage, R.; Finke, A. D.; Linden, A.; Baldridge, K. K.; Siegel, J. S. *Angew. Chem. Int. Ed.* **2016**, *55*, 14648–14652. (b) Mejuto, C.; Escobar, L.; Guisado-Barrios, G.; Ballester, P.; Gusev, D.; Peris, E. *Chem. Eur. J.* **2017**, *23*, 10644–10651. (c) Yokoi, H.; Hiroto, S.; Sakamaki, D.; Seki, S.; Shinokubo, H. *Chem. Sci.* **2018**, *9*, 819–824.

(4) Xu, Y.-Y.; Tian, H.-R.; Li, S.-H.; Chen, Z.-C.; Yao, Y.-R.; Wang, S.-S.; Zhang, X.; Zhu, Z.-Z.; Deng, S.-L.; Zhang, Q.; Yang, S.; Xie, S.-Y.; Huang, R.-B.; Zheng, L.-S. *Nat. Commun.* **2019**, *10*, 485, DOI 10.1038/s41467-019-08343-6.

(5) Gakh, A. A. Molecular Devices, **2018**, Wiley, Hoboken, NJ 07030, USA, Chapt. 5, Molecular Tweezers, pp 213-310.

(6) Recent examples: (a) Barbero, H.; Ferrero, S.; Alvarez-Miguel, L.; Gomez-Iglesias, P.; Miguel, D.; Alvarez, C. M. *Chem. Commun.* **2016**, *52*, 12964−12967. (b) Kuragama, P. L. A.; Fronczek, F. R.; Sygula, A. *Org. Lett.* **2015**, *17*, 5292−5295. (c) Kumarasinghe, K. G. U. R.; Fronczek, F. R.; Valle, H. U.; Sygula, A. *Org. Lett.* **2016**, *18*, 3054−3057. (d) Yang, D.-C.; Li, M.; Chen, C.-F. *Chem. Commun.* **2017**, *53*, 9336−9339.

(7) Recent examples: (a) Gotfredsen, H.; Holmstrøm, T.; Muñoz, A. V.; Storm, F. E.; Tortzen, C. G.; Kadziola, A.; Mikkelsen, K. V.; Hammerich, O.; Nielsen, M. B. *Org. Lett.* **2018**, *20*, 5821−5825. (b) Fukui, N.; Kim, T.; Kim, D.; Osuka, A. *J. Am. Chem. Soc.* **2017**, *139*, 9075−9088. (c) Yoshida, K.; Osuka, A. *Chem. Eur. J.* **2016**, *22*, 9396–9403. (d) Wang, Y.; Uchihara, K.; Mori, S.; Furuta, H.; Shimizu, S. *Org. Lett.* **2019**, *21*, 3103−3107.

(8) Reviews: (a) Sun, M.; Müllen, K.; Yin, M. *Chem. Soc. Rev.* **2016**, *45*, 1513−1528. (b) Würthner, F.; Saha-Möller, C. R.; Fimmel, B.; Ogi, S.; Leowanawat, P.; Schmidt, D. *Chem. Rev.* **2016**, *116*, 962−1052. (c) Nowak-Król, A.; Würthner, F. *Org. Chem. Front.* **2019**, *6*, 1272–1318.

(9) (a) Calvo-Gredilla, P.; García-Calvo, J.; Cuevas, J. V.; Torroba, T.; Pablos, J.-L.; García, F. C.; García, J.-M.; Zink-Lorre, N.; Font-Sanchis, E.; Sastre-Santos, A.; Fernández-Lázaro, F. *Chem.–Eur. J.* **2017**, *23*, 13973–13979.

(10) García-Calvo, J.; Calvo-Gredilla, P.; Ibáñez-Llorente, M.; Romero, D. C.; Cuevas, J. V.; García-Herbosa, G.; Avella, M.; Torroba, T. *J. Mater. Chem. A* **2018**, *6*, 4416–4423.

(11) Busto, N.; Calvo, P.; Santolaya, J.; Leal, J. M.; Guédin, A.; Barone, G.; Torroba, T.; Mergny, J. L.; García, B. *Chem.–Eur. J.* **2108**, *24*, 11292–11296.

(12) Meng, D.; Liu, G.; Xiao, C.; Shi, Y.; Zhang, L.; Jiang, L.; Baldridge, K. K.; Li, Y.; Siegel, J. S.; Wang, Z. *J. Am. Chem. Soc.* **2019**, *141*, 5402−5408.

(13) Lin, Z.; Li, C.; Meng, D.; Li, Y.; Wang, Z. *Chem. Asian J.* **2016**, *11*, 2695 – 2699.

(14) Álvarez, C. M.; Barbero, H.; Ferrero, S.; Miguel, D. *J. Org. Chem.* **2016**, *81*, 6081−6086.

(15) Fernández-García, J. M.; Evans, P. J.; Rivero, S. M.; Fernández, I.; García-Fresnadillo, D.; Perles, J.; Casado, J.; Martín, N. *J. Am. Chem. Soc.* **2018**, *140*, 17188−17196.

(16) (a) Teraoka, T.; Hiroto, S.; Shinokubo, H. *Org. Lett.* **2011**, *13*, 2532–2535. An alternative synthesis exists: (b) Battagliarin, G.; Li, C.; Enkelmann, V.; Müllen, K. *Org. Lett.* **2011**, *13*, 3012–3015.

(17) (a) Thordarson, P. (http://supramolecular.org). (b) Howe, E. N. W.; Bhadbhade, M.; Thordarson, P. *J. Am. Chem. Soc.* **2014**, *136*, 7505−7516. (c) Thordarson, P. *Chem. Soc. Rev.* **2011**, *40*, 1305–1323. (d) Hibbert, D. B.; Thordarson, P. *Chem. Commun.* **2016**, *52*, 12792–12805. (e) Ulatowski, F.; Dąbrowa, K.; Bałakier, T.; Jurczak, J. *J. Org. Chem.* **2016**, *81*, 1746−1756.

(18) Zhao, Y.; Truhlar, D. G. *Theor. Chem. Acc.* **2008**, *120*, 215–241.

(19) *Gaussian 09, Revision D.01*, Frisch, M. J.; Trucks, G. W.; Schlegel, H. B.; Scuseria, G. E.; Robb, M. A.; Cheeseman, J. R.; Scalmani, G.; Barone, V.; Petersson, G. A.; Nakatsuji, H.; Li, X.; Caricato, M.; Marenich, A.; Bloino, J.; Janesko, B. G.; Gomperts, R.; Mennucci, B.; Hratchian, H. P.; Ortiz, J. V.; Izmaylov, A. F.; Sonnenberg, J. L.; Williams-Young, D.; Ding, F.; Lipparini, F.; Egidi, F.; Goings, J.; Peng, B.; Petrone, A.; Henderson, T.; Ranasinghe, D.; Zakrzewski, V. G.; Gao, J.; Rega, N.; Zheng, G.; Liang, W.; Hada, M.; Ehara, M.; Toyota, K.; Fukuda, R.; Hasegawa, J.; Ishida, M.; Nakajima, T.; Honda, Y.; Kitao, O.; Nakai, H.; Vreven, T.; Throssell, K.; Montgomery, Jr., J. A.; Peralta, J. E.; Ogliaro, F.; Bearpark, M.; Heyd, J. J.; Brothers, E.; Kudin, K. N.; Staroverov, V. N.; Keith, T.; Kobayashi, R.; Normand, J.; Raghavachari, K.; Rendell, A.; Burant, J. C.; Iyengar, S. S.; Tomasi, J.; Cossi, M.; Millam, J. M.; Klene, M.; Adamo, C.; Cammi, R.; Ochterski, J. W.; Martin, R. L.; Morokuma, K.; Farkas, O.; Foresman, J. B.; Fox, D. J. Gaussian, Inc., Wallingford CT, **2013**.

(20) (a) Mao, H. K.; Bell, P. M.; Shaner, J. W.; Steinberg, D. J.; *J. Appl. Phys.* **1978**, *49*, 3276-3283. See also: (b) Zou, Y.; Zhang, H. *J. Alloys Compd.* **2019**, *790*, 164-169.

(21) (a) Rao, A. M.; Eklund, P. C.; Hodeau, J-L.; Marques, L.; Nunez-Regueiro, M. *Phys. Rev. B* **1997**, *55*, 4766-4773. See also: (b) Peschanskii, A. V.; Glamazda, A. Yu.; Fomin, V. I.; Karachevtsev, V. A. *Low Temp. Phys.* **2012**, *38*, 854-862.